

Origin of Contractile Force during Cell Division of Bacteria

Biplab Ghosh^{1,2} and Anirban Sain^{1,*}

¹*Physics Department, Indian Institute of Technology–Bombay, Powai, Mumbai, 400076, India*

²*Theoretical Physics Division, Bhabha Atomic Research Center, Trombay, Mumbai 400085, India*

(Received 17 October 2007; published 20 October 2008)

When a bacterium divides, its cell wall at the division site grows radially inward like the shutter of a camera and guillotines the cell into two halves. The wall is pulled upon from inside by a polymeric ring, which itself shrinks in radius. The ring is made of an intracellular protein FtsZ (filamenting temperature sensitive Z) and thus is called the Z ring. It is not understood how the Z ring generates the required contractile force. We propose a theoretical model and simulate it to show how the natural curvature of the FtsZ filaments and lateral attraction among them may facilitate force generation.

DOI: [10.1103/PhysRevLett.101.178101](https://doi.org/10.1103/PhysRevLett.101.178101)

PACS numbers: 87.15.A–, 05.40.–a, 87.15.R–, 87.16.–b

In a wide class of bacteria and some plant cells, the Z ring is believed [1,2] to be the generator of the contractile force needed for its cell division. A 3 μm long and 1 μm wide typical *E. coli* bacterium divides [see Fig. 1(a)] every half hour, of which the contraction phase (cytokinesis) lasts for nearly 10 min [3]. Interestingly, cytokinesis in eukaryotes occur via the constriction of actin ring [4], but there contractile tension is generated due to the interaction between actin filaments and motor proteins, which, however, are absent in the Z-ring system. We propose a mechanism for *E. coli* that involves interaction among filamenting temperature sensitive Z (FtsZ) molecules, anchor proteins, guanosine triphosphate (GTP), and curved membrane, and can lead to a self-propelled contraction of the Z ring. Our model crucially depends on the natural curvature of FtsZ filaments, lateral attraction among them, and GTP hydrolysis. We note that force generation in microtubule filaments, during chromosome segregation in eukaryotes, has been recently explained [5] using intrinsic curvature of the filaments.

Important mechanochemical properties of the FtsZ protein are as follows: (a) FtsZ is a GTPase; i.e., it binds and hydrolyzes GTP to guanosine diphosphate (GDP) [6]. (b) It can polymerize [7] and can further organize into bundles, sheets, and even minirings [8–10], depending on *in vitro* conditions. GTP rich environment enhances polymerization and bundling, while excess GDP favors depolymerization and single strandedness. (c) An FtsZ filament prefers to be straight when its units are bound to GTP, but hydrolysis of GTP to GDP induces curvature in the filament [11–14], although the preferred radius of curvature (R_0) varies (12.5–100 nm) [8,9], depending on the environment. Also the Z ring is very dynamic. It continuously exchanges monomers or protofilaments with the cytoplasm, with an average turnover time $t_{1/2} = 8\text{--}30$ sec [1,15], which is controlled by GTP hydrolysis rate [15].

We now describe our model and qualitatively explain how the Z ring generates force in our model. As shown in Fig. 1(c), the anchors enforce a large radius of curvature

($R_0 \sim 0.5 \mu\text{m}$) on the Z ring by holding it close to the cell membrane. So the filaments of the ring are strained since their intrinsic curvature is much different ($R_0 \sim 12.5\text{--}100$ nm for FtsZ-GDP and $R_0 \gg 0.5 \mu\text{m}$ for FtsZ-GTP). Despite this strain the FtsZ-GTP filaments, which predominately makes the ring [16] are stabilized due to lateral attraction among the filaments. The anchors too add to the stability. But when the outermost layer of the ring begins to get hydrolyzed, the resulting FtsZ-GDP segments would prefer to bend to attain its small intrinsic radius R_0 . But its GTP dependent binding to the ring through its unhydrolyzed segments does not allow immediate bending, instead generates strain (higher than that of FtsZ-GTP) and thus contractile tension in the outermost layer. This tension is transmitted to the cell wall as a contractile radial force through the anchors [Fig. 1(e)]. Note that the curvature dependent strain energy breaks the symmetry between the inner and the outer peripheries of the ring as they differ in curvature. Now the tension in the hydrolyzed FtsZ layer is not due to an elongational strain as in a stretched rubber band (which could be released by shrinkage); the strain is due to FtsZ-GDP's intrinsic bending rigidity. So one way to release it is to detach (depolymerize) the hydrolyzed segments from the ring [Fig. 1(e)]. Later, we show how this hydrolysis induced strain energy controls the attachment and detachment rates of filaments at the peripheral layers of the ring leading to a net contraction in its radius.

We model FtsZ filaments as semiflexible polymers with intrinsic curvature [17]. The filament is described by position vector $\vec{r}(s)$, $s \in [0, L]$ with curvature energy, $H = \frac{\eta}{2} \int_0^L [1/R(s) - 1/R_0]^2 ds$. Here L is the length of the filament, η the bending rigidity, $1/R(s) = |d^2\vec{r}(s)/ds^2|$ the local curvature, and $1/R_0$ is the intrinsic curvature. The Z ring may have the shape of a 3D torus of lateral thickness 20–40 nm [3], but to focus on its radial contraction, here we model it as a bundle of concentric filaments forming a flat annular disc (see Fig. 1), perpendicular to the long axis of the rod-shaped bacteria. The filaments fit on the ring as circular arcs, stabilized by lateral attraction. Henceforth we indicate FtsZ-GTP and FtsZ-GDP by T and D , respec-

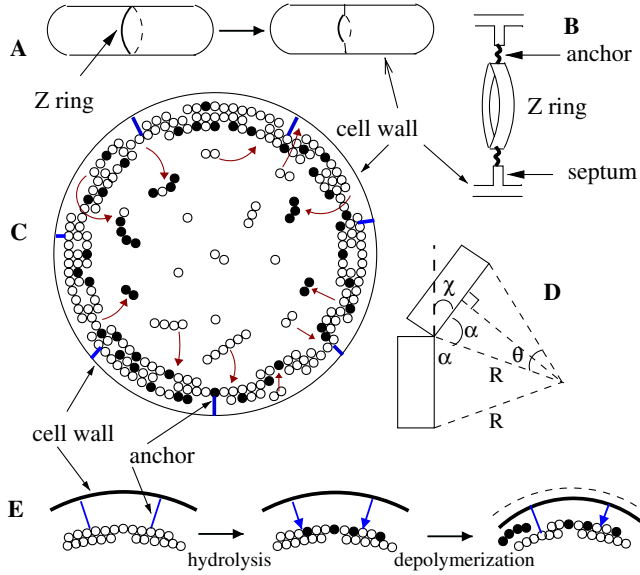


FIG. 1 (color online). (a) Dividing bacteria with contracting Z ring. (b) Schematic drawing of the Z ring anchored to the cell wall. (c) The ring is modeled by a multilayered structure; only three layers are shown, but in our simulation we start with 6–9 layers [15]. GTP-FtsZ and GDP-FtsZ are indicated by open (T) and filled (D) circles, respectively. Oligomers and monomers from the cytoplasm can poly- and depolymerize in and out, from both the inner and the outer peripheries of the ring. (d) FtsZ monomers which are shown as circles in (c), are actually blocks of size $l \sim 5$ nm each, with intermonomer angles χ . A TT pair prefers being straight, while DT or DD pairs prefer finite bending angles. From geometry, intermonomer angle $\chi = \theta$, the angle that a monomer of length l subtends at the center of the ring. $l/R \simeq \chi$ for $l \ll R$ and thus description in terms R or χ are equivalent [5]. (e) shows how partial hydrolysis induces strain in FtsZ filaments and produces radial contraction of the ring. The strained filaments generate radially inward, contractile force (shown by arrows) on the wall (since the radial derivative of its curvature energy is negative). The filament cannot depolymerize immediately and release its strain because of its competing lateral binding, although partially weakened, to the core layers of the ring.

tively. For our simulation results, in Figs. 2 and 3, we assumed two different bending angles, or equivalently R_0 's, for different sets of neighbors: $R_{DD} = R_{DT} = 50$ nm, and $R_{TT} = \infty$ (i.e., no bending). For a filament, which sits on the ring as a circular arc, $R(s)$ is constrained but R_0 varies depending on neighbors. $H(R)$ then reduces to a sum over bonds between neighbors. We include two more energy scales, (a) polymerization energy $-\sigma$ when a filament gets elongated by one monomer, and (b) lateral attraction energy $-\epsilon$ between T 's in radially adjacent layers. Further, since polymerization is more favored with excess GTP than with excess GDP [7,9,10], we set $\sigma_{TT} = -4k_B T$, $\sigma_{DT} = \sigma_{DD} = -k_B T$. We also set $\epsilon = -k_B T$ to allow a weak lateral attraction between T filaments [9,12]. An important effect of this GTP dependent attraction is that fresh T, TT, TTT, \dots are discouraged from attaching onto the ring unless the hydrolyzed $D,$

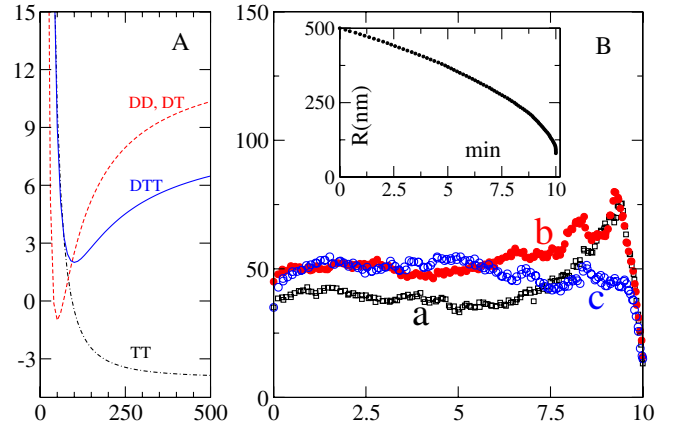


FIG. 2 (color online). (a) Energies $E(R)$ (in $k_B T$) of dimers and trimers versus R (nm), the radius of the layer to which it is bound to, in the Z ring. $E(R)$ includes the curvature energy and the polymerization energy, both of which are composition dependent. Energies of all other trimers (TTT, DDD, TDT , etc.) and oligomers can be inferred from the ones which are plotted. Contributions from lateral attraction energy (ϵ) are not included in $E(R)$ since it depends on the number of occupied sites in the radially neighboring layers. The plot indicates that T oligomers (TT, TTT, \dots , etc.) have lesser energy when they are bound to the ring compared to when they are free in the cytoplasm. For example, while passing from the cytoplasm to the ring a TT dimer loses on curvature energy [$=E(R) - \sigma_{TT} < k_B T$, for $R \geq 150$ nm] but gains more in lateral attraction energy ($2\epsilon = -2k_B T$). It further gains in polymerization energy if it finds neighbors on the same layer of the Z ring on which it lands. While for D -rich oligomers (DD, DT, DDT , etc.) the situation is just the opposite: their energy reduces when they depolymerize from the ring. (b) Shows average ring thickness (nm) versus time (min) for three separate runs, with different parameter sets a, b , and c . The inset shows average outer radius (R) of the ring versus time and sets a, b, c gave similar decay profiles. Sets a, b, c differ in hydrolysis rate, number of layers started with, and ratio of polymers to monomer in the poly- and depolymerization trials. All the runs took nearly 7×10^5 MC steps and were calibrated to total 10 min of contraction time.

DD, DT, DTD , etc., depolymerize from its exposed layers. This not only influences the polymerization rate but also allows very few D 's to get into the core of the ring (see Fig. 3). As a result the ring consists of mostly T 's, consistent with experimental observation [16]. We set bending modulus $\eta = 14000k_B T$ nm, comparable to that of actin ($\sim 17000k_B T$ nm).

We performed a Monte Carlo (MC) simulation on a circular spatial grid, starting with a preformed ring. In poly- and depolymerization trials we allowed both monomers and oligomers (up to 12-mers, in decreasing proportion) to attach to or detach from sites chosen randomly on both the inner and outer periphery of the ring. Polymerization trials involved T, TT, TTT, \dots strands only while depolymerization involved all possible strand compositions ($D, T, DD, TD, TT, DTD, \dots$). Polymerization on the ring followed rules for cooperative growth, i.e., one strand

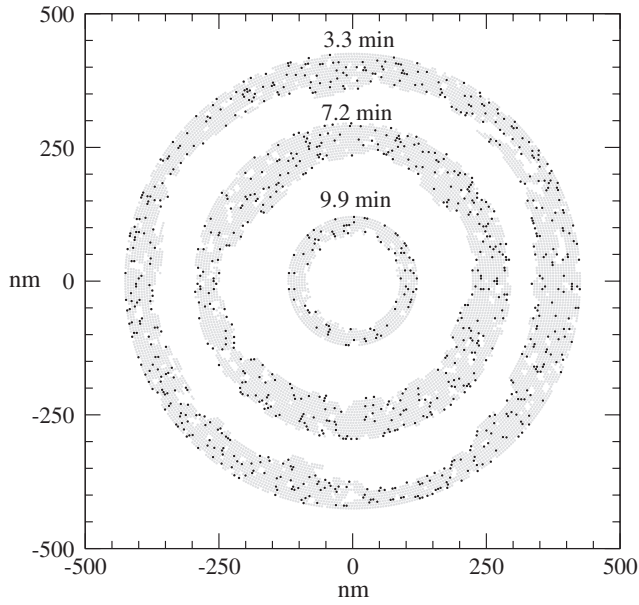


FIG. 3. Time evolution of the Z ring, started at $t = 0$, typically with 6–9 layers, with outer radius 500 nm and with 10% of the FtsZ units at its inner and outer periphery assigned as FtsZ-GDP. A movie [23] captures the full contraction ($R = 500 \text{ nm} \rightarrow 100 \text{ nm}$). Gray and black dots denote T and D , respectively.

growing over another strand and resulting in double or multistranded polymer bundles [11]. Isodesmic growth, i.e., elongation of isolated strands [11], on the other hand, was assumed to maintain the pool of protofilaments in the cytoplasm. Our MC simulation used the Metropolis algorithm with acceptance probability equal to $\exp(-\Delta E/k_B T)$. Energy difference $\Delta E \equiv \Delta(H_{\text{curv}} + E_{\text{poly}} + E_{\text{lateral}})$ includes all sources of energy. Interlayer diffusion was also allowed; i.e., monomers were allowed to hop to vacant sites on interior layers to maximize their coordination numbers and thereby smoothen hills and fill up crevices on the exposed surface.

Polymerization was assumed to be independent of the cytoplasmic density of FtsZ, since a large pool, nearly 70% of approximately 15 000 cellular FtsZ, is available in the cytoplasm [15], and this fraction increases as the ring sheds off more than it absorbs during contraction. Further, a high diffusion constant of order few $\mu\text{m}^2/\text{sec}$ ensures spatial homogeneity. The effect of the anchors were simulated indirectly: during the simulation, every time 80% of the sites in the outermost layer became vacant due to depolymerization, we deleted the grid points on that layer and advanced the cell wall inward by one layer [4].

Once the ring is formed and stabilized by anchors and attractive lateral interactions, it offers a template for further attachment of FtsZ monomers and protofilaments. Similarly depolymerization also occurs from both the exposed inner and outer layers of the ring. The kinetics of attachment and depolymerization depends on the energetics. Random hydrolysis of the exposed monomers in both the inner and outer layers of the ring generates local

contractile stress in the layers since the curvature energies of DT , DD are higher compared to TT at the core. The stress is transmitted to the cell wall through the anchors. The D -rich archs (D , DD , DT , DDD , DTD , $DDDT$, etc.) eventually depolymerize. Note that the D -rich archs at the outermost layer have higher curvature energy than the ones at the innermost layer. So the depolymerization rate at the outer layers are relatively higher. However, attachments of protofilaments T , TT , TTT , ... are energetically favored on both inner and outer layers, almost equally (till $R \geq 150 \text{ nm}$), because lateral attraction overcomes curvature energy. For a fairly broad range of parameters (η , ϵ , σ) it dynamically emerges that despite equal rates of poly- and depolymerization trials at both the peripheries, the net polymerization rate is higher than the depolymerization rate at the inner periphery, and the opposite at the outer periphery. The net effect is disassembly of the outer periphery and assembly at the inner periphery; thus the ring contracts through treadmilling.

In our simulation the ring shrinks monotonically with time [Fig. 2(b), inset] qualitatively in the same fashion found in experiments [18]. We allow hydrolysis at the ring's exposed peripheries at a rate $\sim 3/\text{min}/\text{FtsZ unit}$, comparable to the *in vitro* measured rate ($\sim 5/\text{min}/\text{FtsZ unit}$) [15,16].

In the FRAP (fluorescence recovery after photobleaching) experiments with the Z ring [15], recovery occurs when the bleached FtsZ units on the peripheral layers depolymerize and fresh units from the cytoplasm fill the vacated sites. We interpret the turnover time ($t_{1/2}$) as the average time to depolymerize one layer (from the outer periphery) or to add one fresh layer (at the inner periphery). Parameters (η , σ , ϵ) are adjusted to achieve a dynamical steady state where the two time scales are nearly equal and, consequently, the radial thickness of the ring remains nearly same [Fig. 2(b)] during the major part of the contraction. We obtain $t_{1/2} \approx 14 \text{ sec}$.

It is difficult to estimate the contractile force produced by the ring accurately without knowing the organization of the anchors and how it couples to the various layers of the ring. The septum growth, against an internal pressure of 3 atm, is also accompanied by peptidoglycan (material for the septum) synthesis which can facilitate, and in particular, reduce the force needed for constriction [19]. From our model the maximum contractile tension that can be generated by a fully hydrolyzed D layer is $\mathfrak{S} = H(R)/2\pi R = \frac{\eta}{2} \left(\frac{1}{R_0} - \frac{1}{R} \right)^2$. For the outermost layer of the initial Z ring ($R = 500 \text{ nm}$), assuming $\eta = 14000k_B T \text{ nm}$ and R_0 in the range [12.5–100 nm], we get $\mathfrak{S} = 3\text{--}185 \text{ pN}$. Thus the maximum radial contractile force due to one layer is $\mathfrak{S}/R \sim 0.4 \text{ pN/nm}$. This force can pull out a 1.3 nm wide circular strip of total area $\sim 4000 \text{ nm}^2$ ($= 2\pi \cdot 500 \times 1.3 \text{ nm}^2$) from the membrane against 3 atm internal pressure of the bacteria [see Fig. 1(b)]. If the Z ring is 30 nm thick [3] in the axial direction (i.e., 6 filaments) it can pull out approximately $\sim 8 \text{ nm}$ wide membrane strip.

Peptidoglycan synthesis further widens the thickness of the initial septum. Our formula above indicates that the force decreases with radius; the same qualitative trend has been estimated for animal cell division also [20].

In our simulation, the thickness of the contracting ring turns out to be very sensitive to the hydrolysis rate [Fig. 2(b)]. A decrease (increase) in hydrolysis rate thickens (disintegrates) the ring. This is because in our model hydrolysis not only controls the depolymerization rate (it increases when hydrolysis rate increases), but the higher hydrolysis rate also slows down polymerization (and converse). This is because a rapid hydrolysis rate saturates the peripheries of the ring with D 's and then fresh T monomers and oligomers cannot attach to the peripheries, in the absence of the T -dependent stabilizing lateral attraction. These trends qualitatively agree with *in vivo* observations. For example, (a) a small increase in temperature ($30^\circ\text{C} \rightarrow 42^\circ\text{C}$) is known to disassemble the Z ring [15]. This may be because the *in vivo* hydrolysis rate increases with temperature. (b) For mutant FtsZ84 cells with very slow (10% of wild type) GTPase activity [15], the population of FtsZ in the ring increases from 30% to 60%, which is the same as our ring thickening. Of course, various rates, *in vivo*, could also be dynamically controlled by other divisome proteins.

The existence of the straight to curved transition in FtsZ filaments, due to hydrolysis, has been questioned recently [21]. So we also explored the case where both FtsZ-GDP and FtsZ-GTP have the same intrinsic curvature ($R_0 = 50\text{ nm}$). We recover a similar contraction phenomenon, albeit in a different region of the parameter space: $\eta = 8000k_B T\text{ nm}$, $\epsilon = -2k_B T$, $\sigma_{TT} = -10k_B T$, $\sigma_{DT} = -7k_B T$, $\sigma_{DD} = -2k_B T$, and obtained $t_{1/2} \sim 11\text{ sec}$. These (η , ϵ , σ) values are close to some recent estimates [22]. Recently electron cryotomography data [13] showed that, in *C. crescentus* bacteria, short, disjoint FtsZ filaments are scattered over a wide division region instead of forming a bundle (the Z ring). But it was pointed out that *E. coli* having 3 times more FtsZ than *C. crescentus*, that too localized in a narrow region (along the cylindrical z axis), may not share the same Z-ring structure. In fact, recently artificial Z rings have been reconstituted [14] using membrane targeted FtsZ molecules inside phospholipid membrane tubules. These perfectly round rings can constrict too, at least partially, in the presence of GTP. A ring can also slide along the tube as a whole, and laterally coalesce with a second ring to make a brighter and tighter ring. This indicates lateral attraction among FtsZ filaments as well as a continuous structure of the Z ring. It has been argued [13] that, at least for bacteria like Mycoplasmas, which possess only a cell membrane and no cell wall, but still constrict via the Z ring, a self-propelled contraction mechanism, such as ours, could be relevant.

In summary, we proposed a model to show how prokaryotic organisms may exploit the physical properties of

its own FtsZ filaments, to devise a finely tuned machinery for its cell division. In particular, we have shown how curvature dependent kinetics of the FtsZ protofilaments give rise to different poly- and depolymerization rates at the peripheries of the Z ring, allowing the ring to shrink via treadmilling of its radial layers [5].

We thank A. Rutenberg, M. Jericho, A. Chowdhury, and D. Das for useful comments, and the Department of Science and Technology, India for financial support. We are indebted to D. Panda for introducing us to this topic.

*asain@phy.iitb.ac.in

- [1] J. Lutkenhaus, Annu. Rev. Biochem. **76**, 539 (2007).
- [2] D. S. Weiss, Mol. Microbiol. **54**, 588 (2004).
- [3] I. D. J. Burdett and R. G. E. Murray, J. Bacteriol. **119**, 1039 (1974).
- [4] D. Biron, E. Alvarez-Lacalle, T. E. Tlusty, and E. Moses, Phys. Rev. Lett. **95**, 098102 (2005).
- [5] M. I. Molodtsov *et al.*, Proc. Natl. Acad. Sci. U.S.A. **102**, 4353 (2005).
- [6] P. de Boer, R. Crossley, and L. Rothfield, Nature (London) **359**, 254 (1992); D. RayChaudhuri and J. T. Park, Nature (London) **359**, 251 (1992).
- [7] D. Bramhill and C. M. Thompson, Proc. Natl. Acad. Sci. U.S.A. **91**, 5813 (1994).
- [8] H. P. Erickson, D. W. Taylor, K. A. Taylor, and D. Bramhill, Proc. Natl. Acad. Sci. U.S.A. **93**, 519 (1996).
- [9] J. Mingorance *et al.*, J. Biol. Chem. **280**, 20909 (2005).
- [10] J. M. Gonzalez *et al.*, J. Biol. Chem. **278**, 37664 (2003).
- [11] L. Romberg, M. Simon, and H. P. Erickson, J. Biol. Chem. **276**, 11743 (2001).
- [12] J. M. Gonzalez *et al.*, Proc. Natl. Acad. Sci. U.S.A. **102**, 1895 (2005).
- [13] Z. Li, M. J. Trimble, Y. V. Brun, and G. J. Jensen, EMBO J. **26**, 4694 (2007).
- [14] M. Osawa, D. E. Anderson, and H. P. Erickson, Science **320**, 792 (2008).
- [15] J. Stricker, P. Maddox, E. D. Salmon, and H. P. Erickson, Proc. Natl. Acad. Sci. U.S.A. **99**, 3171 (2002).
- [16] L. Romberg and T. J. Mitchison, Biochemistry **43**, 282 (2004).
- [17] R. E. Goldstein and S. A. Langer, Phys. Rev. Lett. **75**, 1094 (1995).
- [18] G. Reshes, S. Vanounou, I. Fishov, and M. Feingold, Biophys. J. **94**, 251 (2007).
- [19] G. Lan, C. W. Wolgemuth, and S. X. Sun, Proc. Natl. Acad. Sci. U.S.A. **104**, 16110 (2007).
- [20] D. N. Robinson, G. Cavet, H. M. Warrick, and J. A. Spudich, BMC Cell Biol. **3**, 4 (2002).
- [21] M. A. Oliva, D. Trambaiolo, and J. Lowe, J. Mol. Biol. **373**, 1229 (2007).
- [22] I. Horger *et al.*, Phys. Rev. E **77**, 011902 (2008).
- [23] See EPAPS Document No. E-PRLTAO-101-068843 for additional analysis and discussion and a movie which shows the time evolution of the contracting Z ring. For more information on EPAPS, see <http://www.aip.org/pubservs/epaps.html>.